

Mapping the effects of ozone pollution and mixing on floral odour plumes and their impact on plant-pollinator interactions

Article

Accepted Version

Creative Commons: Attribution 4.0 (CC-BY)

Open Access

Langford, B., Ryalls, J. W. M. ORCID: <https://orcid.org/0000-0003-2015-3605>, Mullinger, N. J., Hayden, P., Nemitz, E., Pfrang, C., Robins, A., Touhami, D., Bromfield, L. M. and Girling, R. D. ORCID: <https://orcid.org/0000-0001-8816-8075> (2023) Mapping the effects of ozone pollution and mixing on floral odour plumes and their impact on plant-pollinator interactions. *Environmental Pollution*. 122336. ISSN 0269-7491 doi: <https://doi.org/10.1016/j.envpol.2023.122336> Available at <https://centaur.reading.ac.uk/112993/>

It is advisable to refer to the publisher's version if you intend to cite from the work. See [Guidance on citing](#).

To link to this article DOI: <http://dx.doi.org/10.1016/j.envpol.2023.122336>

Publisher: Elsevier

All outputs in CentAUR are protected by Intellectual Property Rights law, including copyright law. Copyright and IPR is retained by the creators or other copyright holders. Terms and conditions for use of this material are defined in the [End User Agreement](#).

www.reading.ac.uk/centaur

CentAUR

Central Archive at the University of Reading

Reading's research outputs online

Journal Pre-proof

Mapping the effects of ozone pollution and mixing on floral odour plumes and their impact on plant-pollinator interactions

Ben Langford, James M.W. Ryalls, Neil J. Mullinger, Paul Hayden, Eiko Nemitz, Christian Pfrang, Alan Robins, Dalila Touhami, Lisa M. Bromfield, Robbie D. Girling



PII: S0269-7491(23)01338-6

DOI: <https://doi.org/10.1016/j.envpol.2023.122336>

Reference: ENPO 122336

To appear in: *Environmental Pollution*

Received Date: 5 July 2023

Accepted Date: 6 August 2023

Please cite this article as: Langford, B., Ryalls, J.M.W., Mullinger, N.J., Hayden, P., Nemitz, E., Pfrang, C., Robins, A., Touhami, D., Bromfield, L.M., Girling, R.D., Mapping the effects of ozone pollution and mixing on floral odour plumes and their impact on plant-pollinator interactions, *Environmental Pollution* (2023), doi: <https://doi.org/10.1016/j.envpol.2023.122336>.

This is a PDF file of an article that has undergone enhancements after acceptance, such as the addition of a cover page and metadata, and formatting for readability, but it is not yet the definitive version of record. This version will undergo additional copyediting, typesetting and review before it is published in its final form, but we are providing this version to give early visibility of the article. Please note that, during the production process, errors may be discovered which could affect the content, and all legal disclaimers that apply to the journal pertain.

© 2023 Published by Elsevier Ltd.

1 **Mapping the effects of ozone pollution and mixing on floral odour**
2 **plumes and their impact on plant-pollinator interactions**

3 Ben Langford^{a*}, James M.W. Ryalls^b, Neil J. Mullinger^a, Paul. Hayden^c, Eiko Nemitz^a,
4 Christian Pfrang^{d,e,f}, Alan Robins^c, Dalila Touhami^d, Lisa M. Bromfield and Robbie D.
5 Girling^{b,g}

6 ^aUK Centre for Ecology & Hydrology, Penicuik, Midlothian, EH26 0QB, UK

7 ^bSchool of Agriculture, Policy and Development, University of Reading, RG6 6EU, UK

8 ^cEnFlo, Department of Mechanical Engineering Sciences, University of Surrey, Guildford, GU2
9 7XH, UK

10 ^dDepartment of Chemistry, University of Reading, P.O. Box 224, RG6 6AD, Reading, UK

11 ^eSchool of Geography, Earth and Environmental Sciences, University of Birmingham, B15 2TT, UK

12 ^fDepartment of Meteorology, University of Reading, P.O. Box 243, RG6 6BB, Reading, UK

13 ^gCentre for Sustainable Agricultural Systems, Institute for Life Sciences and the Environment,
14 University of Southern Queensland, Toowoomba, Queensland 4350, Australia

15

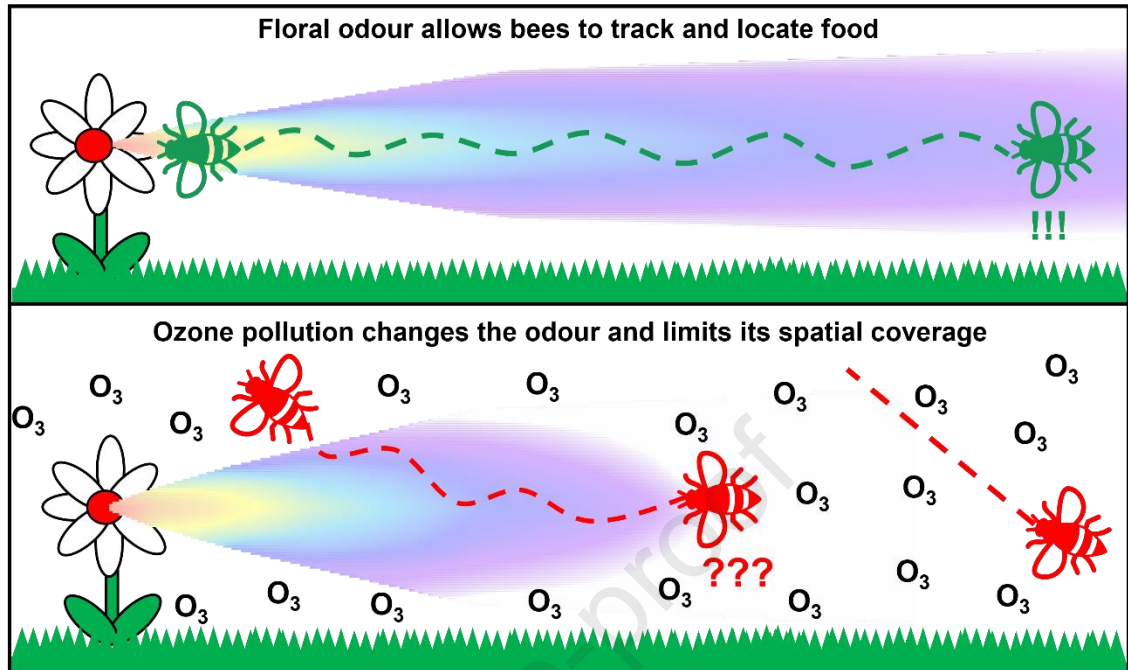
16 *Correspondence: benngf@ceh.ac.uk

17

18 **Highlights:**

- 19
- Ozone pollution degrades the components of floral odour plumes
 - Reaction rates were fastest at the plume edges and slowest at the plume centre
 - Exposure to higher ozone concentrations increased plume intermittency and
22 reduced odour filament width
 - Honeybees recognition of floral odour plumes declined significantly following
24 exposure of the plume to ozone

25 **Graphical Abstract**



26

27 Abstract

28 The critical ecological process of animal-mediated pollination is commonly
 29 facilitated by odour cues. These odours consist of volatile organic compounds (VOCs),
 30 often with short chemical lifetimes, which form the strong concentration gradients
 31 necessary for pollinating insects to locate a flower. Atmospheric oxidants, including ozone
 32 pollution, may react with and chemically alter these VOCs, impairing the ability of
 33 pollinators to locate a flower, and therefore the pollen and nectar on which they feed.
 34 However, there is limited mechanistic empirical evidence to explain these processes within
 35 an odour plume at temporal and spatial scales relevant to insect navigation and olfaction.
 36 We investigated the impact of ozone pollution and turbulent mixing on the fate of four
 37 model floral VOCs within odour plumes using a series of controlled experiments in a large
 38 wind tunnel. Average rates of chemical degradation of α -terpinene, β -caryophyllene and
 39 6-methyl-5-hepten-2-one were slightly faster than predicted by literature rate constants,
 40 but mostly within uncertainty bounds. Mixing reduced reaction rates by 8-10% in the first
 41 2 m following release. Reaction rates also varied across the plumes, being fastest at plume
 42 edges where VOCs and ozone mixed most efficiently and slowest at plume centres.
 43 Honeybees were trained to learn a four VOC blend equivalent to the plume released at
 44 the wind tunnel source. When subsequently presented with an odour blend representative
 45 of that observed 6 m from the source at the centre of the plume, 52% of honeybees
 46 recognised the odour, decreasing to 38% at 12 m. When presented with the more
 47 degraded blend from the plume edge, recognition decreased to 32% and 10% at 6 and 12
 48 m respectively. Our findings highlight a mechanism by which anthropogenic pollutants can
 49 disrupt the VOC cues used in plant-pollinator interactions, which likely impacts on other
 50 critical odour-mediated behaviours such as mate attraction.

51

52

53 **Keywords:** Air pollution, ozone, floral odour cues, insect pollinators, turbulent mixing.

54

55 1. Introduction

56 Floral odours are used by many pollinating insects to locate floral resources. Upon
57 landing on a flower, many species of pollinating insect can learn to associate the unique
58 blend of chemical compounds that make up the flower's odour profile with the nectar
59 reward that it provides, facilitating them to locate rewarding flowers of the same species
60 in the future (Jones and Agrawal, 2017). When an insect uses floral odours to locate a
61 flower, that odour must fulfil certain criteria. For example, it must be relatively short lived,
62 to ensure it does not accumulate, making the cue from individual flowers indistinguishable
63 from the ambient background. At the same time, it must persist for sufficiently long to (i)
64 reach insects and (ii) remain recognisable. Chemical communication is therefore a trade-
65 off between short-lived cues with strong concentration gradients, and long-lived cues that
66 travel further with weak concentration gradients (Williams and Ringsdorf, 2020).

67 Monoterpenes and sesquiterpenes are groups of volatile organic compounds
68 (VOCs) which typically fulfil these criteria and are common components of floral odours
69 (Knudsen et al., 2006). They have relatively short atmospheric lifetimes in the order of tens
70 of minutes to several hours with respect to the hydroxyl radical (OH), the principal oxidant
71 in the troposphere during the daytime, and with respect to NO₃ at night (Atkinson, 2000).
72 Yet, these compounds can also be removed via reactions with ozone (O₃), a powerful
73 oxidant formed at ground level when VOCs and oxides of nitrogen react in the presence
74 of sunlight (Zhang et al., 2019). In the Northern hemisphere background concentrations
75 of O₃ are in the range of 25 to 50 ppb and are further increasing at a rate of between 0.2
76 and 2% per year due to an increase in the emissions of its chemical precursors (Vingarzan,
77 2004), and local pollution episodes can see concentrations in excess of 200 ppb,
78 particularly within or downwind of large conurbations (Group, 2021). For many
79 monoterpenes and sesquiterpenes, reaction with O₃ is more efficient than reaction with
80 OH, resulting in significantly shorter lifetimes. For example, α -terpinene has a lifetime of
81 45 minutes with respect to OH, but less than 30 s when O₃ concentrations exceed 70 ppb
82 (Atkinson et al., 1986).

83 Reaction rates found in the literature assume complete mixing between VOC and
84 oxidant, yet this may not be the case outside of the laboratory. This is particularly true for
85 highly reactive compounds because their chemical lifetime is of the same order as the
86 mixing time scale. This effect of spatial segregation between oxidant and VOC is often
87 overlooked and our understanding of the applicability of reaction rates derived in a
88 laboratory for use in the atmosphere is, therefore, uncertain.

89 An odour plume consists of a series of filaments, which can be considered as
90 strands of higher concentrations of odour, that are formed by turbulent mixing. Recording
91 VOC concentrations at any one stationary point in a plume as it moves and shifts with air
92 movements would reveal bursts of high concentration as a filament is encountered, in-
93 between absences of VOC, defined as the intermittency of the plume (J Murlis et al.,
94 1992). It is this intermittency of signal that an insect's antennae encounters as it attempts
95 to navigate upwind through to the plume's source. The combination of the constituents of
96 an odour plume and its structure are both critical in influencing an insect's in-flight
97 behaviour, enabling it to successfully navigate to the odour source. For example, it is well
98 understood that male moths follow the pheromone plume of a mate by modifying their
99 behavioural responses as a result of the frequency at which they encounter individual
100 odour filaments (Mafra-Neto and Cardé, 1994). Similarly, the plume structure and

101 intermittency of plant and flower odours is important in facilitating the navigation of insects
102 to those odour sources (Beyaert and Hilker, 2014; Riffell et al., 2014).

103 A recent field study using O₃ fumigation by Ryalls et al. (2022) found that the
104 number of pollinators visiting individual flowers declined by 89% when O₃ pollution was
105 elevated above ambient levels. One explanation for this decline was that elevated O₃ may
106 have rapidly degraded components of the floral odour, inhibiting the ability of insects to
107 recognize this odour and successfully locate the flower. This hypothesis was supported
108 by the findings of a mesocosm study on the effects of ozone on the foraging behaviour of
109 the buff-tailed bumblebee, *Bombus terrestris* (Saunier et al., 2023). A second
110 complementary theory, is that air pollutants also cause direct oxidative stress on the
111 insect; studies have demonstrated upregulation of proteins associated with learning and
112 memory in the CNS of honeybees (Reitmayer et al., 2022) and olfactory coding
113 impairment (Démarets et al., 2022). It is therefore likely that both mechanisms play a part.

114 However, there is a gap in the mechanistic empirical evidence to explain how VOC
115 odour degradation by O₃ occurs within an odour plume at temporal and spatial scales
116 relevant to insect navigation and olfaction. To assess the impact of O₃ on the degradation
117 of floral odour plumes a series of experiments were undertaken in a 20 m wind tunnel,
118 modified to allow fumigation by O₃ to predefined levels. The study focused on four VOCs,
119 α -terpinene, β -caryophyllene, 6-methyl-5-hepten-2-one (MHO) and linalool, which are all
120 common components of floral odours (Knudsen et al., 2006), represent a range of
121 atmospheric lifetimes, and have different molecular weights so are distinguishable from
122 one another in real-time using a proton transfer reaction time-of-flight mass spectrometer.
123 Here, we present the results for both a single compound odour plume (α -terpinene) and
124 multicomponent odour plumes (α -terpinene, β -caryophyllene, MHO and linalool) under O₃
125 concentration fields of approximately 0, 50 and 150 ppb. The measured odour plumes are
126 compared against those expected based on literature rate constants at various points
127 within the plumes.

128 In addition, a separate behavioral assay was conducted to assess whether the
129 degradation of odour plumes could affect the ability of honeybees to recognise an odour.

130

131 2. Materials and methods

132

133 2.1 Wind tunnel measurements

134 Measurements were made at the Natural Environment Research Council
135 (NERC) and National Centre for Atmospheric Science (NCAS) wind tunnel facility at the
136 University of Surrey. The Environmental Flow (EnFlo) wind tunnel is a 20 m (L) x 1.5 m
137 (H) x 3.5 m (W), draw down design with the capability of modulating inlet flow temperature
138 and generating specific boundary layer conditions (Carpentieri et al., 2012), (Hancock and
139 Pascheke, 2014). Within the tunnel are two three-dimensional traversing gears, which
140 allow the automation of sampling at specific, predefined locations. The tunnel is equipped
141 with a gas handling system to enable the passive release of trace gases at predefined
142 locations within the tunnel. The first seven meters of the tunnel are used to establish
143 boundary conditions and mixing, leaving approximately 12 m of wind tunnel to perform
144 measurements, with the final 1 m inaccessible to the 3D traverse.

145 A nominally 1 m deep boundary layer was generated in the wind tunnel, using a
146 standard system of triangular spires (Irwin, 1981) and a rough surface. Previous work had
147 established the characteristics of this boundary layer, including the variation of mean
148 velocity, turbulence intensity and turbulence length scales with height. The experiments

149 used two separate release heights, 0.5 and 0.75 m. Lateral and vertical turbulence
150 intensities at the two heights were 4.5 % and 3.2 % for the vertical component and 5.2%
151 and 3.2 % for the lateral: length scales were similar at the two heights being 11% of the
152 boundary layer height of ~ 1 m for the vertical component and 13% for the lateral
153 (Carpentieri and Robins, 2015). Finally, we note that these heights are well above the
154 near-wall, logarithmic region, which extends top about 20% of the boundary layer depth.
155 Further rationale for the wind tunnel setup is given in Section 1.1 of the Supplementary
156 Information (SI).

157

158 2.1.1 Ozone Fumigation

159 The concentration of O_3 inside the wind tunnel was controlled by releasing O_3 from
160 a lattice manifold, which was suspended in front of the upwind air intake of the wind tunnel.
161 The lattice comprised 35 mm diameter PVC tubing to form a 3.5 m by 1.5 m rectangle with
162 four vertical struts at regular (0.67 m) intervals. The tubing had 5 mm diameter holes drilled
163 at 25 mm intervals to allow for an even distribution of the O_3 into the tunnel. The O_3
164 concentration inside the wind tunnel was continuously monitored (2B Technologies, Model
165 202 Ozone Monitor) at a fixed location (see Fig. 1a) with the measured concentration used
166 to feedback to a Proportional–Integral–Derivative (PID) controller which in turn determined
167 the release rate of O_3 from two generators (CD1500P, ClearWater Tech, USA). Working
168 section O_3 levels only reached target concentrations when the entire laboratory that
169 houses the wind tunnel reached steady-state conditions. Two O_3 levels were used: ~ 50
170 ppb during the working-day, based on the ambient air quality standard (60 ppb), and 150
171 ppb at other times, based on the work-place standard (200 ppb). For this reason, the main
172 fumigation experiments were conducted outside of working hours to avoid exposing
173 laboratory users to concentrations exceeding the air quality standard. High frequency (10
174 Hz) measurements were also made using an O_3 monitor (Ecophysics, CLD 88 O_3) and
175 both analysers were calibrated against an O_3 calibration source (2B Technologies, Model
176 306).

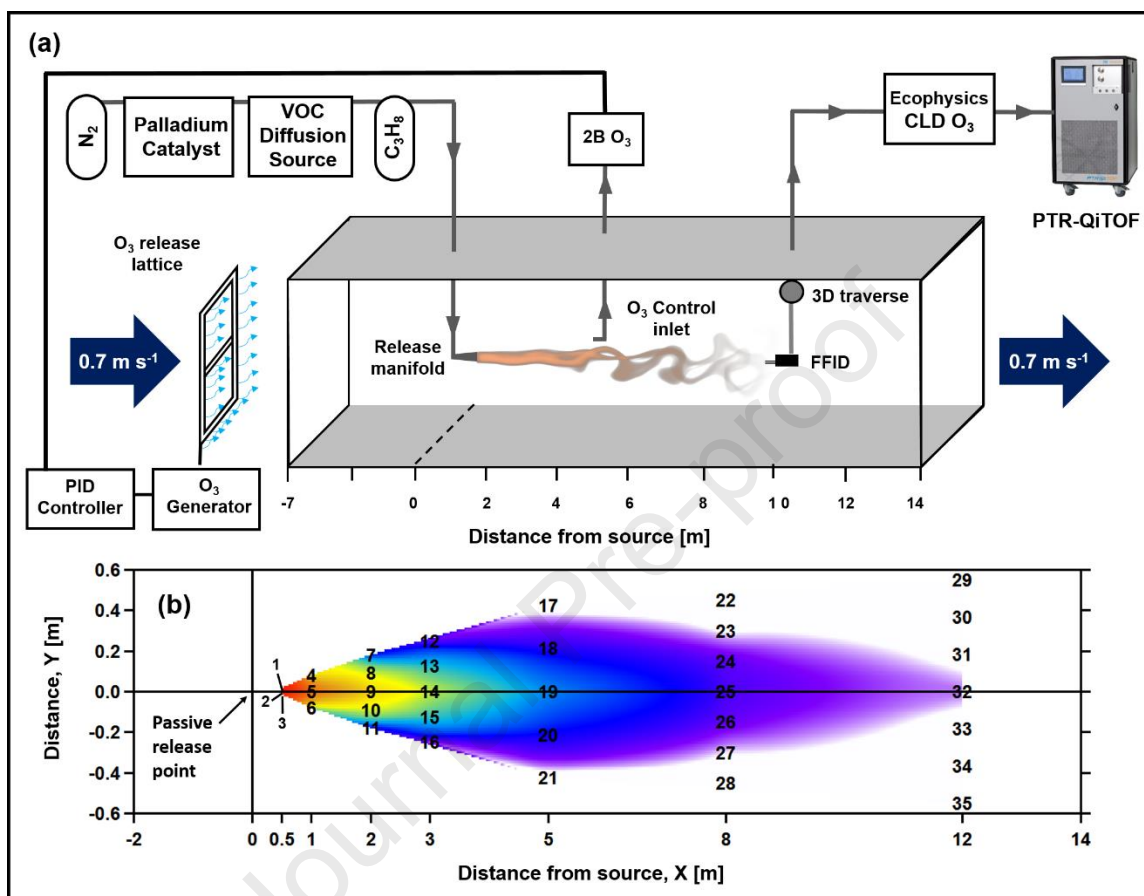
177

178 2.1.2 Simulated floral odour plumes

179 Floral odours were simulated by releasing a blend of five trace gases which
180 ensured consistency throughout and between experiments. These included propane, an
181 inert tracer compound with respect to O_3 (Atkinson, 2000) and four VOCs, α -terpinene, β -
182 caryophyllene, MHO and linalool. Propane was released directly from a gas cylinder,
183 whereas the remaining four compounds were generated using a custom-built diffusion
184 device. Liquid standards of the four compounds were sealed in stainless steel (316 grade)
185 diffusion tubes and placed into one of two stirred water baths (Grant Instruments, TX150,
186 Cambridge). Oxygen free nitrogen was passed through a zero air generator (ZA FID AIR
187 6.0, Uvison Technologies, UK) and then flowed over the diffusion tubes at a rate of 0.3 L
188 min^{-1} . The VOC rich air was subsequently combined with propane (UN1978 Propane,
189 Tech Grade N1.5) and released through a $\frac{1}{4}$ " diameter (O.D.) isokinetic release nozzle at
190 a flow rate of 1 L min^{-1} . This release rate ensured the simulated floral odour exited the
191 manifold at the same velocity as the air in the wind tunnel (~ 0.7 m s^{-1}) ensuring a passive
192 release of the VOCs. The concentration of each VOC closest to the release point (x, y

193 coordinates of 0.5, 0 m, see Fig. 1b) was ~100 ppb for α -terpinene, 6 ppb for β -
 194 caryophyllene, 2.5 ppb for Linalool and 4.5 ppb for MHO.

195



196

197 Figure 1. Schematic of the wind tunnel measurement setup (panel a) and cross-section of the wind tunnel
 198 identifying the positions of the 35 measurement locations used (panel b).

199

200 2.2 Measurement of floral odour

201 2.2.1 Proton transfer reaction – time-of-flight – mass spectrometer

202 The concentration of the VOCs within the simulated floral odour were measured
 203 using a proton transfer reaction time-of-flight mass spectrometer, with quadrupole ion
 204 guide (PTR-QiTOF, Ionicon Analytik GmbH, Austria) (Jordan et al., 2009). The conditions
 205 within the instrument's drift tube were kept constant throughout each experiment with
 206 pressure, temperature and voltage maintained at 3.8 mbar, 80 °C and 860 V, respectively.
 207 This ensured the ratio between electric field and number density of molecules (E/N) within
 208 the drift tube was maintained at 122 Td and that fragmentation of ions remained
 209 consistent. An assessment of ion fragmentation and instrument calibration is shown in
 210 Section S1.2 of the SI.

211 Air was sampled from the wind tunnel at a rate of $\sim 6 \text{ L min}^{-1}$ (at 500 mbar) from a
212 $\sim 25 \text{ m}$ long $\frac{1}{4}$ " O.D (1/8" I.D) PFA sampling line. To avoid sampling at reduced pressures,
213 air for analysis by PTR-QiTOF was subsampled using a Teflon headed pump (KNF) to
214 pass the air past the instrument inlet. The sample line was mounted directly to the three-
215 dimensional traverse inside the wind tunnel and the tube heated to $80 \text{ }^\circ\text{C}$ to limit absorption
216 of VOCs to the tube walls. A PTFE filter ($0.45 \mu\text{m}$ pore size) was placed in line after the
217 pump to prevent particulate matter entering the instrument. The temperature of the air
218 within the sample line was monitored continuously and was to within $1 \text{ }^\circ\text{C}$ of the recorded
219 wind tunnel temperature.

220 A Fast Flame Ionisation Detector (FFID, Cambustion, HFR400) was used
221 to provide highly time resolved measurements of the plume structure. The frequency
222 response of the FFID is 200 Hz and is small enough to be mounted on the traverse. The
223 FFID operates in the range of 1000 to 0.05 ppmv . Air was sampled into the FFID along a
224 350 mm length of steel tubing (O.D. = 0.55 mm). The FFID was calibrated at the start of
225 the experiment and frequent background measurements were made to allow for drift
226 corrections which were on average less than 3% .
227

228 2.2.2 Sampling Protocol

229 Each plume was sampled at 35 separate locations comprising seven horizontal
230 cross sections at $0.5, 1, 2, 3, 5, 8$ and 12 m downwind of the release point (Fig. 1b). Direct
231 measurements at point $0, 0$ (co-ordinates are distances x, y in m relative to the release
232 point and height) were not feasible and therefore measured concentrations at each
233 location in the wind tunnel were always normalised to the 2nd measurement point (e.g. $x =$
234 $0.5 \text{ m}, y = 0 \text{ m}$), which became the effective release point.

235 PTR-QiTOF data were recorded with a time resolution of 10 Hz and sampled at
236 each of the pre-defined locations for 13 minutes. This duration was found to offer a good
237 compromise between obtaining robust statistics and ensuring all measurement locations
238 could be sampled during the time period when O_3 fumigation in the laboratory was
239 permitted. Following each wind tunnel measurement, the background concentration was
240 monitored by sampling at the wind tunnel edge, outside of the plume for 1 minute. The
241 final step was to measure the concentration of VOCs coming from the diffusion source for
242 1 minute, to ensure any minor deviations in release concentration could be corrected. In
243 total, each plume characterisation experiment took approximately 9 hours to complete.

244 2.3 Plume intermittency and odour filament width

245 The intermittency of an odour plume is defined here as the fraction of time (0-1)
246 the VOC concentration falls below the threshold of perception (ToP). This threshold is
247 insect dependent, so here an arbitrary value defined as 1% of the 98th percentile of
248 observed concentrations was used. The width of individual odour filaments was calculated
249 by counting the number of consecutive measurements falling below the ToP at each
250 location within the wind tunnel and averaging the results. The sampling rate of the PTR-
251 QiTOF was 10 Hz and, therefore, each measurement was equivalent to a filament width
252 of 0.1 s .

253 2.4 Proboscis extension response assay

254 To establish the effects of O₃ induced changes to the composition of floral odours
255 on a pollinating insect's ability to successfully recognise that odour, proboscis extension
256 response (PER) assays were performed using the western honeybee (*Apis mellifera*).

257 Liquid standards of the four VOCs used in the wind tunnel study were mixed into
258 a blend, with volumes initially based on the vapour pressure of each compound (Table
259 S1). Concentrations were assessed using a solid phase microextraction fibre (SPME) in
260 combination with GC-MS and the methods used are outlined in Section 1.3 of the SI.
261 Having established the initial ratio of the blend, two sets of three further odour blends were
262 prepared aiming to replicate the ratios observed in the wind tunnel under the 150 ppb
263 treatment at distances of 2, 6 and 12 m from the source. The first set represented the
264 ratios seen in the plume centre and the second represent those seen at the plume edge.
265 SPME collection and GC/MS analysis were repeated on two random blends to ensure that
266 individual compounds were within 2% of the calculated fractions.

267 Proboscis Extension Response assays were conducted in an air-conditioned room
268 at ca. 21 °C, lit by artificial light, with O₃ concentrations always at background levels (<10
269 ppb (Nazaroff and Weschler, 2022)). Returning forager honeybees were collected from
270 the entrance of a hive maintained on the University of Reading's Whiteknights campus
271 (51° 26' 9" N, 0° 56' 25" W). Individual worker bees were immobilised by cooling them on
272 ice in 60 mL containers before being transferred and harnessed into a 1 ml pipette tip
273 (Felsenberg et al., 2011). Only honeybees showing an initial PER elicited by 1.5 M sucrose
274 solution were used. Each honeybee was trained to associatively learn the source VOC
275 blend (α -terpinene, β -caryophyllene, MHO and linalool in a 1:1:1:1 ratio). Following the
276 protocol of Matsumoto et al. (2012), honeybees were acclimatised to a continuous flow
277 (650 mL min⁻¹) of charcoal-filtered humidified air for 25 s before being presented with the
278 4 s conditioned odour stimulus (i.e. an odour stream from a glass pipette containing filter
279 paper impregnated with 20 μ L of the source blend). This was immediately followed by a 3
280 s sucrose stimulation (unconditioned stimulus; 1.5 M sucrose solution) with a 1 s overlap,
281 regulated by a CS-55 V2 stimulus controller (Syntech, The Netherlands). Honeybees were
282 left in the air stream for a further 25 s after sucrose delivery to ensure that no contextual
283 cues around the setup would be associated with the unconditioned stimulus. Honeybees
284 were scored as having learnt the source blend if a proboscis extension was observed
285 between odour onset and sucrose delivery. The learning trial was repeated four times for
286 each honeybee and the inter-trial interval for each honeybee was 10 min. In the
287 recognition trials the responses of 77 honeybees were tested to each of the six odour
288 blends that had been prepared to replicate the VOC ratios recorded in the wind-tunnel
289 experiments at either 2, 6 or 12 m from the source at either the plume centre or the plume
290 edge. Recognition trials mirrored the conditioning trials, with the omission of sucrose.
291 Extension of the proboscis within 4 s in response to the onset of the odour stimulus was
292 classified as a positive recognition. The procedure was followed by the presentation of the
293 source blend (0 m). Honeybees that did not extend their proboscis in response to the final
294 conditioned stimulus ($N = 6$ of 77) were excluded from analysis. As such, 34 and 37
295 individuals responding to VOC blends at the plume centre and plume edge, respectively
296 (71 honeybees in total), were incorporated in statistical analyses (see Section 1.4 of the
297 SI).

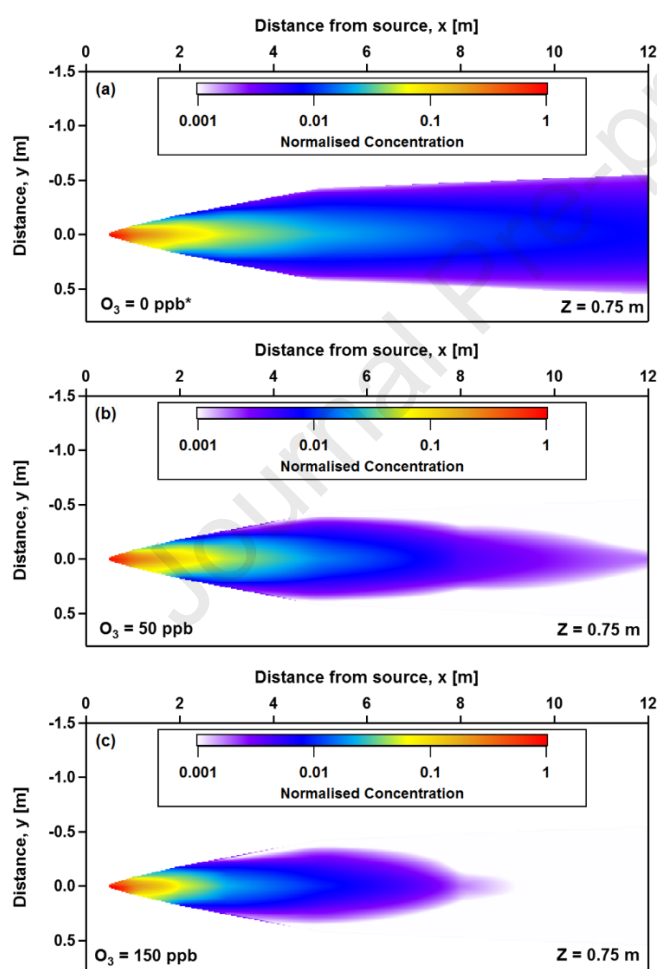
298

299

300 **3. Results and discussion**301 **3.1 Wind tunnel plume measurements**302 *3.1.1 α -terpinene plume*

303 A single component release of α -terpinene was used to map out the spatial
 304 distribution of an odour plume and to determine how this changed under differing levels of
 305 O_3 pollution. Figure 2 shows the measured odour plumes under O_3 fields of 0 (Fig. 2a), 50
 306 (Fig. 2b), and 150 ppb (Fig. 2c). Background O_3 levels within the wind tunnel were between
 307 8 and 12 ppb and therefore a true 0 ppb field could not be achieved. Instead, Fig. 2a
 308 shows a plume of propane, which does not react with O_3 and can therefore be considered
 309 representative of the α -terpinene plume injected into a zero O_3 concentration field.

310



311

312 **Figure 2. Horizontal plume cross sections showing the concentration of α -terpinene normalised to the point closest**
 313 **to the odour plume source for ozone (O_3) fields of ~0 (panel a), ~50 (panel b) and ~150 ppb (panel c). The colour**
 314 **scale of each plume has been log normalised. * Panel a shows a plume of propane, which does not react with O_3**
 315 **and can, therefore, be considered representative of the α -terpinene plume injected into a zero O_3 concentration**
 316 **field.**

317

318 Each plot consists of the 35 individual measurement points (shown in Figure 1b)
 319 which have subsequently been interpolated using the “natural neighbour” approach and
 320 Voroni tessellation (See “image_interpolate” function, Igor Pro, Version 8.0.3.3,
 321 Wavemetrics). Similar plots showing the average O₃ concentration are shown in the
 322 Supplementary Information (figure S1).

323 For each experiment the wind tunnel was operated using a standard 1 m boundary
 324 layer. which resulted in a wind speed of 0.68 m s⁻¹ at the 0.75 m height and 0.63 m s⁻¹ at
 325 the 0.5 m measurement height, equivalent to travel times of ~16.9 and 18.25, respectively,
 326 between the effective release point and the end of the wind tunnel. Figure 2a, where no
 327 ozonolysis occurs, demonstrates the effect of dilution on the plume, concentrations
 328 dropping to < 1% of the effective release point by the time the air exits the wind tunnel.

329 The addition of O₃ to the wind tunnel changed the plume shape causing a
 330 narrowing as the α -terpinene mixed with the O₃ rich air at the plume edges. Figure 2b
 331 shows that ozonolysis removed almost all of the α -terpinene in the 16 s that it took for plume
 332 to travel the length of the wind tunnel at 50 ppb of O₃, and at 150 ppb (Fig. 2c), all of the
 333 α -terpinene had reacted away by 9.5 m (13.5 s). These two-dimensional cross sections
 334 demonstrate how a plumes spatial extent, both length and width, can be significantly
 335 reduced under increasing levels of O₃ pollution at concentrations regularly observed in the
 336 lower troposphere at background levels (50 ppb) and also during elevated pollution
 337 episodes (150 ppb) (Group, 2021).

338 The α -terpinene plumes were also modelled by subtracting the expected chemical
 339 loss from the conserved propane plume. Theoretical first-order loss rates were calculated
 340 as

$$341 \quad Loss = \left(\frac{t}{t_{loss}} \right), \quad (2)$$

342 where t is the time since release into the O₃ field in seconds and t_{loss} is the total
 343 loss rate of VOC with respect to O₃ calculated as

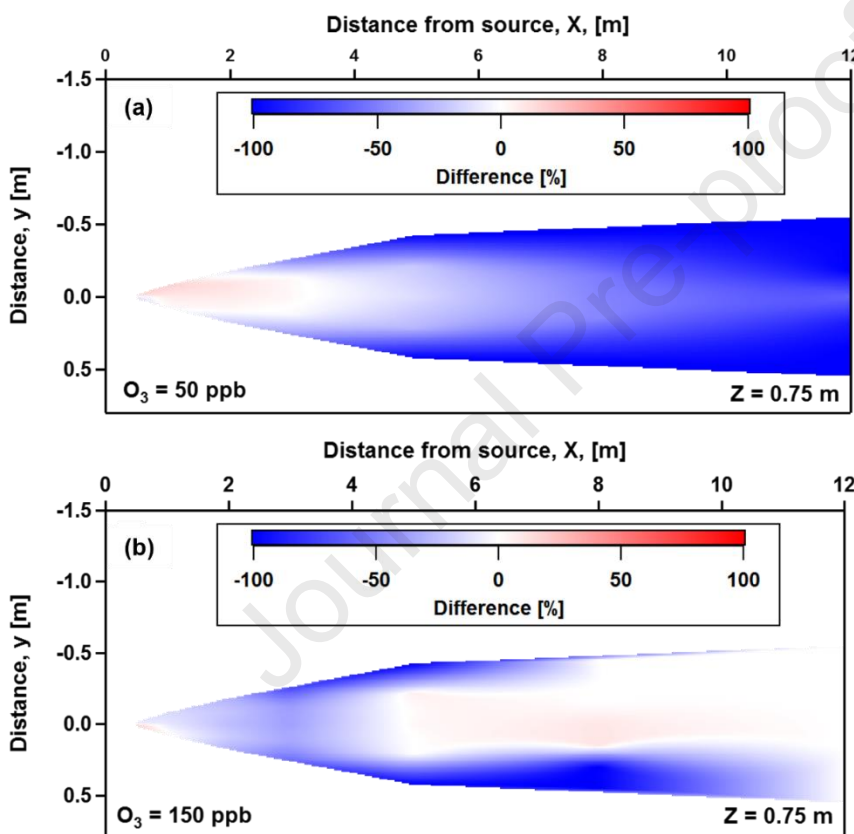
$$344 \quad t_{loss} = \left(\frac{(k_{AT,O_3})^{-1}}{[O_3]} \right). \quad (3)$$

345 Here, k_{AT,O_3} , is the ozonolysis rate constant (see Table S1) and [O₃] was the
 346 concentration of O₃ measured at each location in the wind tunnel in molecules cm⁻³. The
 347 time since release was calculated based on the straight-line distance between the
 348 effective release and measurement point and the fixed wind speed.

349 Figure 3, panels a and b show the percentage difference between measured and
 350 theoretical plumes for the ~50 and ~150 ppb O₃ fields, respectively. In both cases, the
 351 measured plume is degraded more quickly than would be expected based on the literature
 352 rate constant: an average of 21% for 50 ppb and 24% for 150 ppb, based on the measured
 353 data points, only. This was partially explained by the additional time available for reaction
 354 as sampled air was drawn into the PTR-QiTOF. A cross-covariance function applied to the
 355 propane signal measured *in situ* by the FFID (and used for the theoretical plume
 356 calculations) and PTR-QiTOF showed this delay to be ~1.6 s (see Figure S2 of the SI).

357 Accounting for this additional delay reduced the average difference to 18% and 12%, for
 358 50 ppb and 150 ppb scenarios, respectively.

359 The overall increased reaction rates may be influenced by additional chemical
 360 sinks in the wind tunnel including reactions with either OH or NO₃, which were not
 361 measured during the study. The spatial behaviour of the plume supports the view that
 362 imperfect mixing affects the rate constant: the difference plots highlight the increased
 363 reaction rate at the plume edges, where mixing between O₃ and the VOC is particularly
 364 efficient, but less change is seen at the plume centre. The reaction rate appears slowest
 365 during the first 0.5 to 2 m after release, which is consistent with the limited opportunity for
 366 mixing shortly after release. Incomplete mixing reflects the intensity of segregation
 367 between the O₃ and VOCs,



368
 369 Figure 3 shows the percentage difference between an a-terpinene plume predicted based on literature rate
 370 constants and that measured by the PTR-QiTOF (e.g. measured – predicted)/predicted). Panel a and b show the
 371 difference plot under ozone conditions of 50 ppb and 150 ppb of ozone, respectively. Both plumes were released
 372 from a height of 0.75 m.

373

374

375 which effectively reduces the rate constant and increases the lifetime of the compound.
 376 The rate of change of VOC concentration with respect to O₃ can be calculated as

$$377 \quad \frac{\partial[VOC]}{\partial t} = -k_{VOC,O_3}([O_3][VOC] + [O_3']VOC'), \quad (4)$$

378 where square brackets represent averages and the primes denote deviations from the
 379 mean concentration. Using the measured α -terpinene and O_3 concentrations, both
 380 measured at 10 Hz, the effective rate coefficient (k_{eff,AT,O_3}) can be calculated following the
 381 approach of Krol et al. (2000) and Pugh et al. (2010), where the intensity of segregation,
 382 S , between O_3 and α -terpinene is defined as

$$383 \quad S_{AT,O_3} = \frac{[O_3'AT']}{[O_3][AT]}. \quad (5)$$

384 This intensity of segregation can be used to derive an effective rate constant as:

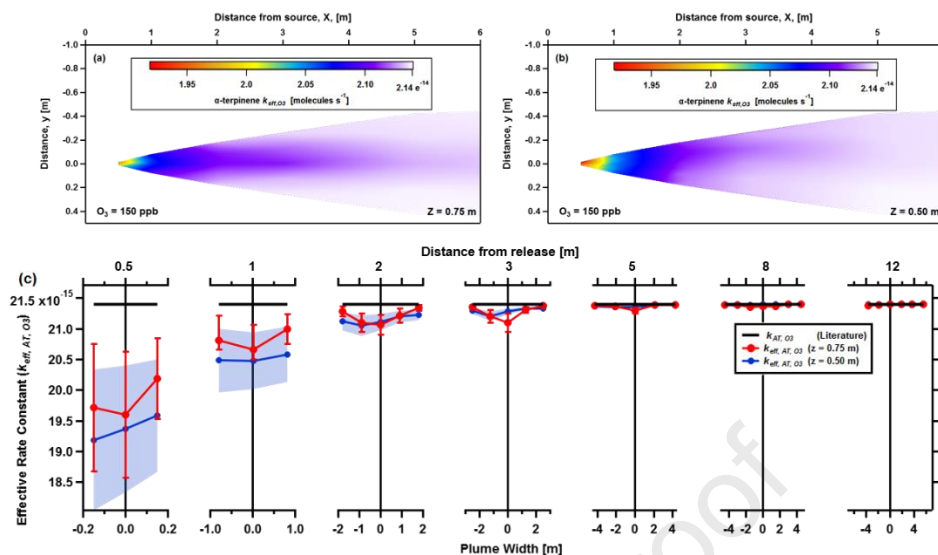
$$385 \quad k_{eff,AT,O_3} = k_{AT,O_3}(1 + S_{AT,O_3}). \quad (6)$$

386 Figure 4, panel (a) shows the effective rate constant for α -terpinene, calculated
 387 based on the α -terpinene plume released at a height of 0.75 m into an O_3 field of 150 ppb.
 388 The literature rate constant for α -terpinene is $2.1 \times 10^{-14} \text{ cm}^3 \text{ molecule}^{-1} \text{ s}^{-1}$, and the
 389 effective rate constant is roughly equivalent to this at the plume centre between 4 and 8
 390 m. However, at the effective release point ($y=0$, $x=0.5$), k_{eff,AT,O_3} is decreased by $\sim 8\%$,
 391 thereby increasing the lifetime of α -terpinene at that point. Towards the plume edges, from
 392 3 m down the tunnel and beyond, k_{eff,AT,O_3} is closer to k_{AT} , than at the plume centre where
 393 there the α -terpinene has less opportunity to mix with the O_3 .

394 Repeating the same experiment at the lower height of 0.5 m (Figure 4b), where
 395 turbulence is slightly increased, showed a somewhat steeper gradient in the effective rate
 396 constant, with up to a 10% reduction at the effective release point. This is counter to
 397 expectation because the increased turbulence and longer travel time should enhance
 398 mixing and reduce the effects of segregation. Figure 3c shows the effective rate constant
 399 for both measurement heights at each location within the tunnel. There is a small
 400 difference between the effective rate constants measured at 0.5 and 1 m but this was
 401 within the uncertainty bounds which was based on the standard deviation of the
 402 measurements. This potentially reflects the fact that differences in the turbulence
 403 intensities between the two heights was relatively minor (4.5 % and 3.2 % for the vertical
 404 component and 5.2% and 3.2 % for the lateral). Further measurements at lower heights
 405 were not possible due to the potential for the plume to interact with the wind tunnel's
 406 surface.

407 A maximum 8-10% decrease of the rate constant may appear modest, but it should
 408 be viewed as a lower limit. This is because our instruments were limited to a frequency
 409 response of 10 Hz. Comparison of the PTR-QiTOF measurements with those of propane
 410 made by the FFID at a frequency of 200 Hz, revealed fine scale variation in concentration
 411 that is lost when using a 10 Hz measurement (see Fig. S3). Therefore, the effects of
 412 segregation could be greater; particularly for an insect encountering the plume, whose
 413 antennae can detect changes at a rate far greater than 10 Hz (Szyszka et al., 2014).

414 This result indicates that mixing plays an important, but often overlooked, role in
 415 the lifetime of VOCs. For those VOCs used as chemical cues, this is particularly important
 416 because the short lifetimes necessary to generate strong concentration gradients mean
 417 the lifetime of the signal compound is invariably similar to, or shorter than, the mixing time
 418 scale.



419

420 Figure 4. The effective rate constant (k_{eff,O_3}) for α -terpinene measured at 0.75 m (panel a) and
 421 ground level when released into an ozone field of 150 ppb. Panel b) shows the measured effective rate constant at
 422 each point within the wind tunnel at the two measurement heights together with the uncertainty (red line = 0.75 m,
 423 blue line = 0.5 m). The literature rate constant, k_{O_3} , is 2.14×10^{-14} (black line). Turbulence levels were 3-5% higher
 424 both laterally and vertically for the 0.5 m height.

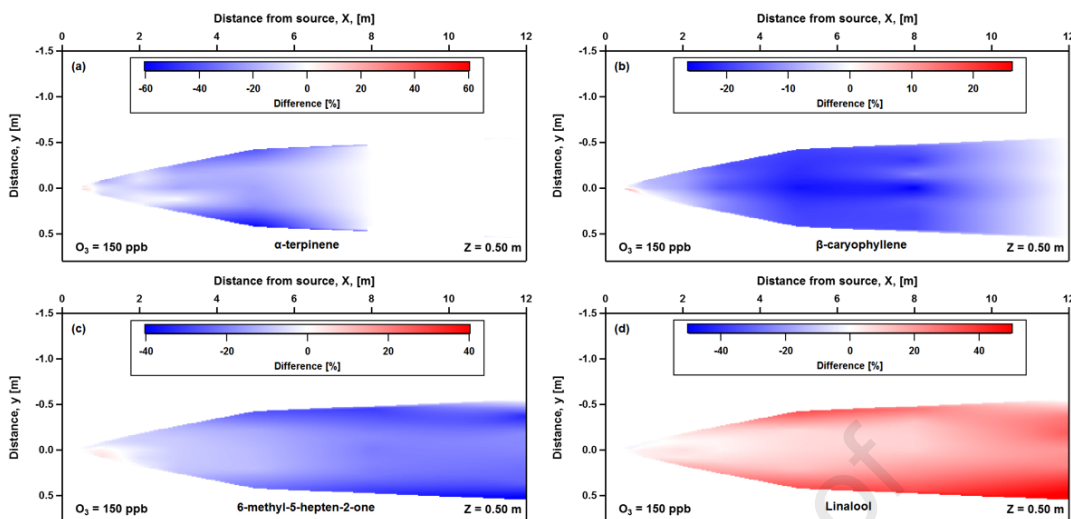
425

426 3.1.2 Multi-component plume

427 Cross sectional plots of each individual component of the multicomponent release,
 428 which is more representative of a floral odour plume, showed variations in the reaction
 429 rates of the four VOCs: α -terpinene, β -caryophyllene, MHO and linalool (see Fig. S4 a-d).
 430 The difference between the theoretical and measured plumes are shown in Figure 5 and
 431 a more detailed comparison that incorporates the uncertainty of the literature rate
 432 constants is shown in Figures S5-S8. For α -terpinene, β -caryophyllene and MHO, the
 433 measured plumes are again degraded faster than would be expected based on their
 434 respective O_3 rate constants, with the largest differences occurring at the plume edge.
 435 Applying a correction for the additional sampling delay accounted for 7% and 4% of the
 436 difference for α -terpinene, β -caryophyllene, respectively, and less than 1% for MHO. As
 437 was the case for α -terpinene, the reason for the reaction rates exceeding those expected
 438 based on literature rate constants, even despite the effects of segregation, likely relates
 439 to the presence of OH and or NO_3 within the wind tunnel.

440 Linalool is degraded more slowly than implied by its rate constant and the
 441 difference becomes larger towards the plume edge. It is likely that an oxidation product,
 442 from either α -terpinene or β -caryophyllene is formed which contributes to the linalool
 443 signal, most likely as a fragment ion. This is supported by the fact that the difference is
 444 largest at the plume edge where the mixing and hence reaction rates are at their fastest.

445



446
447
448
449
450
451
452
453
454
455
456
457
458
459
460
461
462
463
464
465
466
467
468
Figure 5 shows the percentage difference between VOC plumes that has been predicted based on literature reaction rates with O_3 , and that measured by PTR-QiTOF (e.g. (measured – predicted)/predicted) Panel a-d show the results for α -terpinene (a), β -caryophyllene (b), MHO (c) and linalool (d). The odour plume was released from a height of 0.5 m into an ozone field of 150 ppb.

3.2 Effect of ozone on plume intermittency and odour filament width

446
447
448
449
450
451
452
453
454
455
456
457
458
459
460
461
462
463
464
465
466
467
468
Plume intermittency is considered to be a function of source strength and turbulent mixing. Yet. Figure 6 shows that higher levels of O_3 caused an increase in intermittency and reduction in odour filament width of an α -terpinene plume when released under identical turbulent profiles. These changes are likely to have behavioural consequences for a flying insect using the odour plume to navigate to a source. Both factors are critical in eliciting insect flight behaviours and small changes to plume structure can have dramatic effects on flight behaviour and the ability of a foraging insect to locate an odour source (Beyaert and Hilker, 2014; Mafra-Neto and Cardé, 1994) However, we did not directly investigate the effects of the changes we observed to intermittency and filament number on insect flight behaviour and therefore the degree of impact of those changes remains unclear. Again, the largest changes in intermittency and odour filament width were observed towards the outer edges of the plume where mixing with O_3 is most efficient.

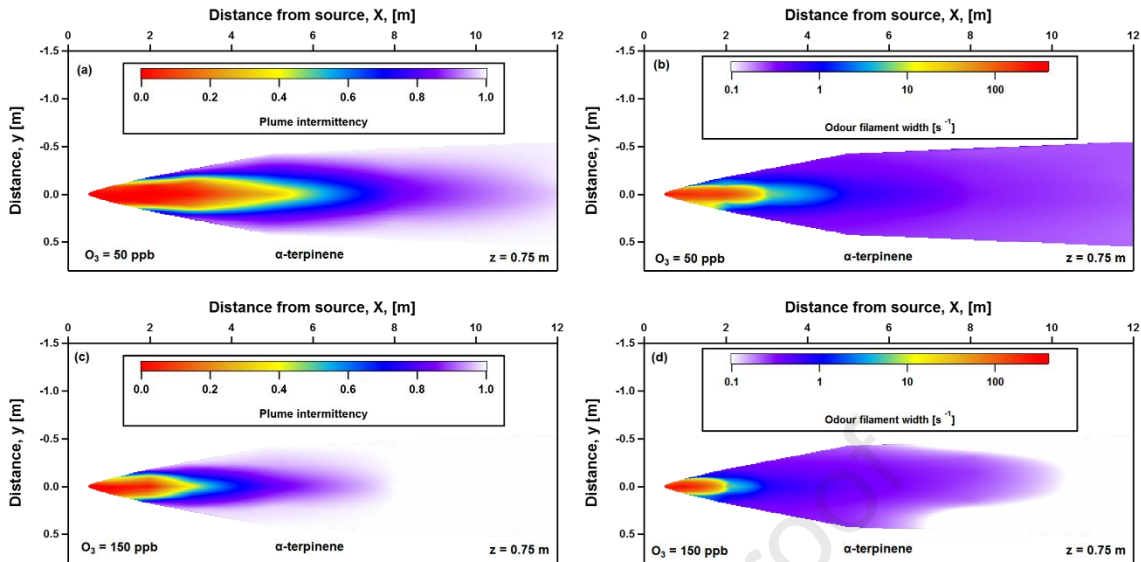


Figure 6, panels a and c, show the intermittency of an α -terpinene plume, defined as the fraction of time (0-1) that the measured signal fell below the threshold of perception (see text for definition), under identical turbulent conditions but varying ozone concentrations of 50 ppb and 150 ppb, respectively. Panels b and d show the average odour filament width from the same α -terpinene plumes. Note the colour scale in panels b and d are shown on a logarithmic scale.

3.3 Honeybee Proboscis Extension Response (PER) Assays

Figure 7 shows the ratios recorded in the wind-tunnel under 150 ppb of O_3 , and those reproduced for the PER assays. Panels a versus c show the plume centre and b versus d show the plume edge. The ratios were not identical but provided a reasonable approximation of the composition change observed in the wind tunnel.

When honeybees were presented with the VOC odour profile they had been trained to (i.e. the profile representative of the VOC blend at the tunnel source, or 0 m), 100% showed a positive PER response (Figure 7 c and d), i.e. all individuals recognised the blend to which they had been trained. However, for the less degraded central plume (figure 7 c), when honeybees were presented with a VOC blend representative of that recorded at 6 m from the tunnel odour source only 52% of honeybees tested exhibited a positive PER response, decreasing to 38% for bees presented with the VOC blend representative of 12 m from the odour source. For the honeybees presented with VOC blends representing the more degraded plume edge (Figure 7 d), just 32% responded to that representing 6 m from the odour source, decreasing to 10% to the blend representing 12 m from the odour source. Overall, significantly fewer honeybees responded to the VOC blend at the plume edge compared with the plume centre ($\chi^2_1 = 9.56$, $P = 0.002$) and significantly fewer honeybees responded as the distance from the source increased ($\chi^2_1 = 39.17$, $P < 0.001$). There was no significant two-way (Location x Distance) interaction ($\chi^2_1 = 9.56$, $P = 0.002$). These results suggests that changes in VOC ratios resulting from O_3 pollution and at fairly small foraging distances from a floral odour source could cause large reductions in the ability of honeybees to be able to recognise a floral blend, potentially disrupting the processes pollinating insects rely on for location of floral food resources. This supports previous findings of behavioural studies, which have

502 demonstrated changes in insect behaviour (Vanderplanck et al., 2021) (Saunier et al.,
503 2023) and reduced pollination of flowers under elevated O₃ (Ryalls et al., 2022).

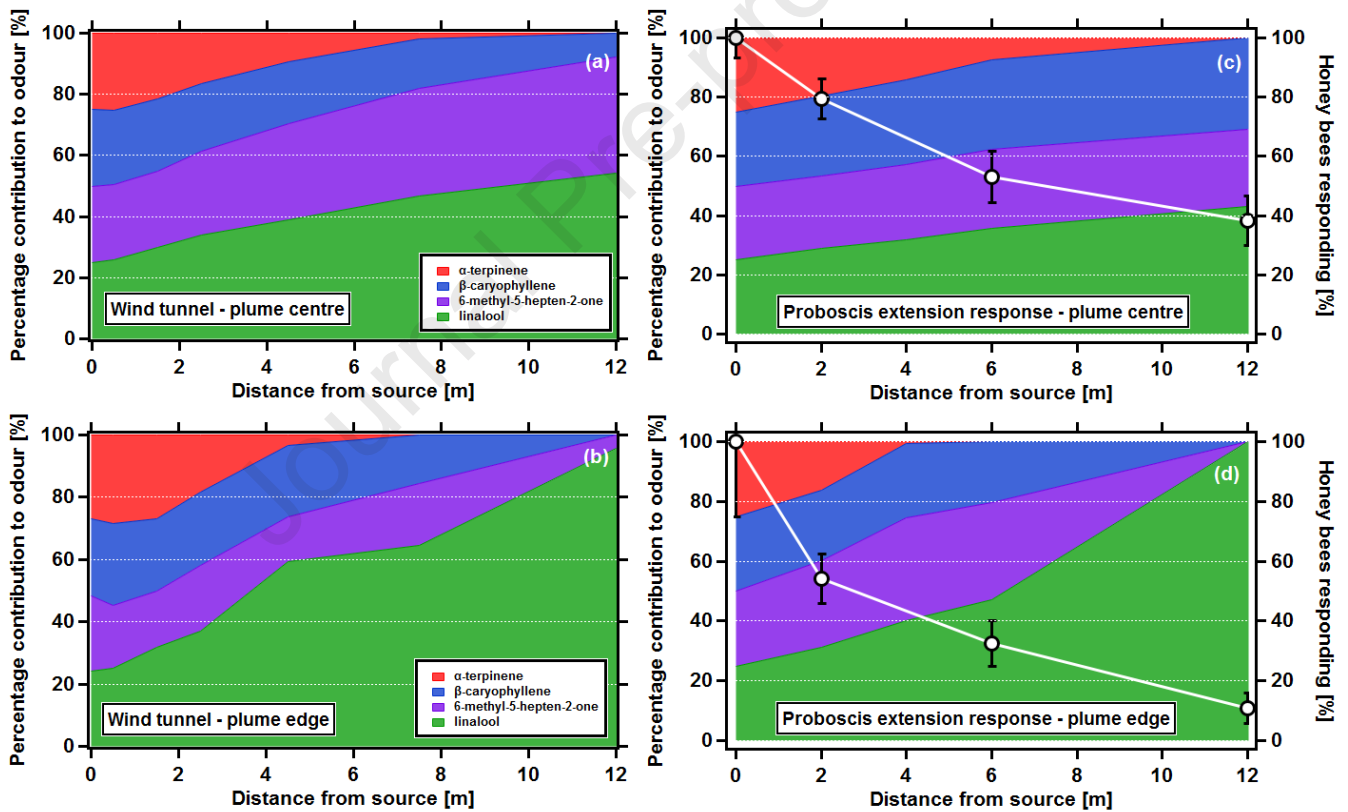
504

505 It should be noted that this assay purely assessed the honeybee's abilities to
506 recognise the odour and therefore, the results do not capture any additional effects
507 associated with direct exposure to O₃. Furthermore, here the honeybees are responding
508 to a mean concentration, and therefore, the additional impact of O₃ on the spatial extent
509 and intermittency of the plume as well as the odour filament width are not captured within
510 the honeybees response.

511

512

513



514

515 Figure 7 Observed ratios of α-terpinene, β-caryophyllene, 6-methyl-5-hepten-2-one (MHO) and linalool measured at
516 the plume centre (panel a) and plume edge (panel b) under an ozone field of 150 ppb. Panels c and d show an
517 attempt to replicate these ratios as part of a proboscis extension response assay, for the plume centre and plume
518 edge, respectively. The right hand axis and line graphs on panels c and d indicate the percentage of forager
519 honeybees which, after learning the four VOC blend representative of 0 m from the source, extended their
520 proboscis (indicating recognition) when presented with VOC blends representative of 2, 6 and 12 m from the source
521 (± S.E.). Data are expressed as the percent PER recognition of each distance relative to the PER recognition of
522 blend at the source ((n = 34 and 37 individuals for the plume centre and plume edge, respectively). While there was
523 no significant two-way interactive effect of 'distance from the source' and 'location of the plume', both were
524 individually significant. As such, significantly fewer honeybees responded to the VOC blend corresponding to the

525 plume edge compared with the plume centre ($z = -2.814$, $P < 0.005$) and honeybee responses significantly decreased
526 from 2 to 6 m ($z = -3.39$, $P = 0.001$) and from 6 to 12 m ($z = -2.82$, $P = 0.005$) according to post-hoc tests.

527

528 4. Conclusions

529 Controlled releases of both single and multiple component synthetic floral odours
530 were measured in a wind tunnel under differing levels of O_3 . The rate of reaction of each
531 compound (α -terpinene, β -caryophyllene, MHO and linalool) were found to be broadly
532 similar to that expected based on literature rate constants, but in most cases slightly faster,
533 likely due to additional chemical sinks (e.g. OH and NO_3) for the VOCs within the wind
534 tunnel. The notable exception was linalool, where reaction rates were slower than
535 expected. In this case, fragmentation of an oxidation product to m/z 155 was thought to
536 be the most likely cause.

537 An analysis of the intensity of segregation between the concentrations of α -
538 terpinene and O_3 revealed that the effective rate constant (k_{eff,AT,O_3}) was reduced by up to
539 10% in the first 2 m following release. The effect of segregation was expected to decrease
540 at lower measurement heights, but no statistically significant difference was observed
541 between the 0.75 and 0.5 m measurements. This reflected the small differences in
542 turbulence intensity between these two measurement heights. Reaction rates were fastest
543 at the plume edges attributed to the increased opportunity to mix with ozone. Ozone was
544 also found to increase the intermittency of the plume and decrease odour filament width,
545 two properties used by insects for navigation.

546 Replication of the average plume composition in a proboscis response assay
547 clearly showed a rapid decline in honeybees' ability to recognise the floral odour following
548 simulated degradation by O_3 . These results, although based upon a synthetic odour,
549 provide an important insight into the mechanism by which anthropogenic pollutants can
550 disrupt the chemical cues used by insects. Importantly, our experimental approach, where
551 the effects of O_3 degradation were replicated and then presented to the insect, allows its
552 effects to be de-coupled from potential olfactory coding impairment caused by direct
553 oxidative stress. In this instance, the effects are pronounced within just a short distance
554 from the point of release.

555 However, outside of the laboratory, the extent to which ozonolysis impacts on
556 pollinators will ultimately depend on the reactivity of the components within a given floral
557 odour, the ambient O_3 concentration (and NO_3 if at night-time) and wind speed.
558 Nonetheless, our work demonstrates a clear mechanism, capable of explaining the large
559 decline in pollinator visits seen in previous field scale O_3 fumigation studies (Ryalls et al.,
560 2022) which may also be relevant for other odour-mediated behaviours such as mate
561 attraction.

562

563 Acknowledgments

564 We thank Paul Nathan and Zoe Ansell for technical support during the wind tunnel studies. Thanks
565 to Helen Dominick for assistance collecting honeybees. Thanks to Dr Stephen Elmore for support
566 during the GC-MS studies.

567

568

569

570 Funding

571 This work was funded by the Natural Environmental Research Council (NERC) through the project
572 Degradation of Odour signals by air pollution: chemical Mechanisms, plume dynamics and Insect-
573 Orientation behaviour (DOMINO, NE/P001971/2) and the PTR-QiToF instrument through
574 grant NE/P016502/1

575

576 Declaration of competing interest

577 The authors declare that they have no known competing financial interests or personal relationships
578 that could have appeared to influence the work reported in this paper.

579

580 Data availability

581

582 Data is available upon reasonable request.

583

584 Author statement

585

586 RG, BL, CP and EN obtained the funding, BL, NJM, DT, RG, CP, EN, PH and AR performed the
587 wind tunnel study. JR, LB and RG performed the proboscis extension response assays and all
588 authors contributed to the writing of the manuscript.

589

590 References

591 Atkinson, R., 2000. Atmospheric chemistry of VOCs and NOx. *Atmospheric Environment* 34,
592 2063-2101.

593 Atkinson, R., Aschmann, S.M., Pitts Jr., J.N., 1986. Rate constants for the gas-phase reactions of
594 the OH radical with a series of monoterpenes at 294 ± 1 K. *International Journal of Chemical*
595 *Kinetics* 18, 287-299.

596 Beyaert, I., Hilker, M., 2014. Plant odour plumes as mediators of plant-insect interactions. *Biol*
597 *Rev Camb Philos Soc* 89, 68-81.

598 Carpentieri, M., Hayden, P., Robins, A.G., 2012. Wind tunnel measurements of pollutant turbulent
599 fluxes in urban intersections. *Atmospheric Environment* 46, 669-674.

600 Carpentieri, M., Robins, A.G., 2015. Influence of urban morphology on air flow over building
601 arrays. *Journal of Wind Engineering and Industrial Aerodynamics* 145, 61-74.

602 Démares, F., Gibert, L., Creusot, P., Lapeyre, B., Proffit, M., 2022. Acute ozone exposure impairs
603 detection of floral odor, learning, and memory of honey bees, through olfactory generalization.
604 *Science of the Total Environment* 827, 154342.

605 Felsenberg, J., Gehring, K.B., Antemann, V., Eisenhardt, D., 2011. Behavioural pharmacology in
606 classical conditioning of the proboscis extension response in honeybees (*Apis mellifera*). *J Vis*
607 *Exp*.

608 Group, A.Q.E., 2021. Ozone in the UK - recent trends and future projections, pp. 1-143.

609 Hancock, P.E., Pascheke, F., 2014. Wind-tunnel simulation of the wake of a large wind turbine in
610 a stable boundary layer. Part 1: the boundary-layer simulation. *Boundary-Layer Meteorology* 151,
611 3+.

- 612 Irwin, H.P.A.H., 1981. The design of spires for wind simulation. *Journal of Wind Engineering and*
613 *Industrial Aerodynamics* 7, 361-366.
- 614 J Murlis, J S Elkinton, a., Cardé, R.T., 1992. Odor Plumes and How Insects Use Them. *Annual*
615 *Review of Entomology* 37, 505-532.
- 616 Jones, P.L., Agrawal, A.A., 2017. Learning in Insect Pollinators and Herbivores. *Annual Review of*
617 *Entomology* 62, 53-71.
- 618 Jordan, A., Haidacher, S., Hanel, G., Hartungen, E., Mark, L., Seehauser, H., Schottkowsky, R.,
619 Sulzer, P., Mark, T.D., 2009. A high resolution and high sensitivity proton-transfer-reaction time-
620 of-flight mass spectrometer (PTR-TOF-MS). *International Journal of Mass Spectrometry* 286,
621 122-128.
- 622 Knudsen, J.T., Eriksson, R., Gershenzon, J., Ståhl, B., 2006. Diversity and distribution of floral
623 scent. *The Botanical Review* 72, 1.
- 624 Krol, M.C., Molemaker, M.J., de Arellano, J.V.G., 2000. Effects of turbulence and heterogeneous
625 emissions on photochemically active species in the convective boundary layer. *Journal of*
626 *Geophysical Research: Atmospheres* 105, 6871-6884.
- 627 Mafra-Neto, A., Cardé, R.T., 1994. Fine-scale structure of pheromone plumes modulates upwind
628 orientation of flying moths. *Nature* 369, 142-144.
- 629 Matsumoto, Y., Menzel, R., Sandoz, J.-C., Giurfa, M., 2012. Revisiting olfactory classical
630 conditioning of the proboscis extension response in honey bees: A step toward standardized
631 procedures. *Journal of Neuroscience Methods* 211, 159-167.
- 632 Nazaroff, W.W., Weschler, C.J., 2022. Indoor ozone: Concentrations and influencing factors.
633 *Indoor Air* 32, e12942.
- 634 Reitmayer, C.M., Girling, R.D., Jackson, C.W., Newman, T.A., 2022. Repeated short-term
635 exposure to diesel exhaust reduces honey bee colony fitness. *Environmental Pollution* 300,
636 118934.
- 637 Riffell, J.A., Shlizerman, E., Sanders, E., Abrell, L., Medina, B., Hinterwirth, A.J., Kutz, J.N., 2014.
638 Flower discrimination by pollinators in a dynamic chemical environment. *Science* 344, 1515-1518.
- 639 Ryalls, J.M.W., Langford, B., Mullinger, N.J., Bromfield, L.M., Nemitz, E., Pfrang, C., Girling, R.D.,
640 2022. Anthropogenic air pollutants reduce insect-mediated pollination services. *Environmental*
641 *Pollution* 297, 118847.
- 642 Saunier, A., Grof-Tisza, P., Blande, J.D., 2023. Effect of ozone exposure on the foraging
643 behaviour of *Bombus terrestris*. *Environmental Pollution* 316, 120573.
- 644 Szyszka, P., Gerkin, R.C., Galizia, C.G., Smith, B.H., 2014. High-speed odor transduction and
645 pulse tracking by insect olfactory receptor neurons. *Proceedings of the National Academy of*
646 *Sciences* 111, 16925-16930.
- 647 Vanderplanck, M., Lapeyre, B., Brondani, M., Opsommer, M., Dufay, M., Hossaert-McKey, M.,
648 Proffit, M., 2021. Ozone Pollution Alters Olfaction and Behavior of Pollinators. *Antioxidants* 10,
649 636.

650 Vingarzan, R., 2004. A review of surface ozone background levels and trends. Atmospheric
651 Environment 38, 3431-3442.

652 Williams, J., Ringsdorf, A., 2020. Human odour thresholds are tuned to atmospheric chemical
653 lifetimes. Philosophical Transactions of the Royal Society B: Biological Sciences 375, 20190274.

654 Zhang, J., Wei, Y., Fang, Z., 2019. Ozone Pollution: A Major Health Hazard Worldwide. Frontiers
655 in Immunology 10.

656

657

658

659

660

661

662

663

664

665

666

667

668

669

670

671

672

673

674

675

676

677

678

679

680

Highlights:

- Ozone pollution degrades the components of floral odour plumes
- Reaction rates were fastest at the plume edges and slowest at the plume centre
- Higher O₃ levels increased plume intermittency and reduced odour filament width
- Bees recognition of floral odours declined significantly following reaction with O₃

Journal Pre-proof

Declaration of interests

The authors declare that they have no known competing financial interests or personal relationships that could have appeared to influence the work reported in this paper.

The authors declare the following financial interests/personal relationships which may be considered as potential competing interests:

Journal Pre-proof